

Very shallow geothermal potential in urban areas: parameterization algorithm and mapping tool for thermal conductivity and thermal resistivity in Warsaw (Poland)

Mateusz ŻERUN^{1,*}, EWA JAGODA², Edyta MAJER¹ and Krzysztof MAJER¹

¹ Polish Geological Institute – National Research Institute, Jagiellońska 76, 03-301 Warszawa, Poland; ORCID: 0000-0002-6824-5624 [M.Ż.], 0000-0001-8489-2357 [E.M.], 0000-0001-7284-1739 [K.M.]

² University of Warsaw, Faculty of Geology, Żwirki i Wigury 93, 02-089 Warszawa, Poland; ORCID: 0000-0002-7453-9362 [E.J.]



Żeruń, M., Jagoda, E., Majer E., Majer, K., 2025. Very shallow geothermal potential in urban areas: parameterization algorithm and mapping tool for thermal conductivity and thermal resistivity in Warsaw (Poland). Geological Quarterly, **69**, 55; <https://doi.org/10.7306/gq.1828>

Associate Editor: Beata Jaworska-Szulc

The transition toward Smart City development relies on efficient integration of digital and geoscientific data to improve the sustainability of urban infrastructure. A key component of this process is the optimal utilization of subsurface thermal resources for clean energy systems, as well as the planning of underground infrastructure. This study presents a novel adaptation of the national Engineering-Geological Database of Poland (BDGI) for mapping the very shallow geothermal potential of urban areas. Using more than 35,000 boreholes from the Warsaw region, the database was processed to generate spatial models of thermal conductivity () and thermal resistivity () at depths from 2 to 30 m below ground level. The shallow thermal conductivity maps so prepared are particularly relevant for the design of energy geostructures (e.g., geothermal piles, thermoactive foundations, energy tunnels) and horizontal ground heat exchangers. The data shown as thermal resistivity maps can also support the design and operation of urban transmission infrastructures such as district heating, electricity, and water networks. The case study area is characterized by loose sediments and soils (compressive strength R_c ~ 600 kPa, according to ISO 14689), while solid rocks were not considered as they do not occur at such shallow depths. The resulting thermal maps provide new insights into the spatial variability of the urban subsurface and constitute a practical geospatial tool for energy and infrastructure planning in sustainable city development.

Key words: very shallow geothermal potential, thermal parameters of rock and soil, geological databases, urban geothermal.

INTRODUCTION

The transition toward a low-carbon energy system requires a significant increase in the share of renewable energy sources (RES) in Poland's energy mix, in line with national, EU, and international climate policies. Low-temperature geothermal energy fits perfectly into this framework, providing a stable and continuous source of renewable heat. Ground-source heat pump (GSHP) systems can be effectively used for heating, cooling, seasonal energy storage, and waste heat recovery, thereby reducing low-stack emissions and improving urban air quality and energy efficiency.

Urban areas are of particular importance in the transition being undertaken. They possess the highest energy demand

densities but also face spatial constraints that limit the installation of new energy systems (Goetzl et al., 2023). Continuous urban expansion driven by transport, residential and commercial development creates an opportunity to exploit the interaction between buildings and the ground for shallow geothermal use. The growing extent of underground structures, such as car parks, metro tunnels, and foundations, provides potential surfaces for heat exchange with the surrounding soil (Baralis et al., 2018; Barla et al., 2020).

In this context, thermoactive geostructures, including energy piles, diaphragm walls, foundation slabs and tunnel linings, represent a promising direction in sustainable building design. When typically equipped with embedded polyethylene tubing, these structural elements can function as ground heat exchangers, using circulating fluids (water or water-glycol mixtures) to transfer heat between the subsurface and the building (Ciapala et al., 2025). The efficiency of such systems depends mainly on the thermal properties of the ground, particularly thermal conductivity () and thermal resistivity (), as well as the heat pump's coefficient of performance (COP) (Loveridge et al., 2020; Hou et al., 2022). Reliable knowledge of subsurface thermal conditions is therefore a prerequisite for optimizing the de-

* Corresponding author, e-mail: mateusz.zerun@pgi.gov.pl

Received: October 13, 2025; accepted: December 2, 2025; first published online: January 10, 2026

sign and performance of very shallow geothermal energy (vSGE) systems.

While thermal conductivity governs the rate of heat transfer through the soil or rock matrix, thermal resistivity represents its inverse, describing the resistance of the ground to heat flow. High resistivity values indicate poor heat dissipation capacity and can lead to local overheating or thermal inefficiencies in buried systems (Enescu et al., 2021). In the context of energy and utility infrastructure, understanding the spatial variability of thermal resistivity is as important as conductivity. Subsurface layers with low thermal resistivity values are favourable for heat dissipation, which is critical for the safe and efficient operation of underground power cables, pipelines, and district heating networks. Conversely, areas with higher resistivity may require design adaptations or active cooling strategies. Hence, thermal resistivity mapping supports both geothermal system design and thermal risk assessment for buried utilities, contributing to more sustainable and resilient underground space management.

In Poland, this research area remains insufficiently developed. National and regional geothermal atlases have been published for deep geothermal resources, as well as for shallow systems suitable for vertical ground heat exchangers (typically 40–130 m b.g.l.), accompanied by a defined methodology for resource assessment (Górecki et al., 2006a, b, 2011, 2012, 2013; Ryżyński et al., 2023). There are still no detailed, spatially continuous maps of very shallow geothermal potential (vSGP) for the upper 30 metres of the subsurface. Moreover, a standardized methodology for such mapping has not yet been developed. Data on the thermal properties of soils and unconsolidated deposits, which are essential for the design of energy foundations, horizontal ground heat exchangers, and subsurface energy transport systems, remain fragmented and largely inaccessible. This knowledge gap limits the integration of very shallow geothermal and thermal management solutions into urban energy and infrastructure planning. Our research builds upon an earlier conceptual framework presented by Źeruń et al. (2024), expanding its scope through enhanced data integration, inclusion of thermal resistivity analyses, and detailed spatial interpretation for the Warsaw metropolitan area.

To address this issue, the present study introduces a workflow for mapping vSGP based on the Engineering-Geological Database of Poland (BDGI). The database is maintained by the Polish Geological Institute – National Research Institute and is the largest national repository of digital data on engineering and geological conditions. It contains nearly 500,000 boreholes drilled and recorded between 1998 and 2023, including over 35,000 from the Warsaw metropolitan area. The subsurface of Warsaw is composed almost entirely of unconsolidated Quaternary and Pliocene deposits, mainly sands, silts, and clays, classified as soils with compressive strength R_c 600 kPa (ISO 14689). Solid rocks do not occur within the top 30 metres and were therefore excluded from the analysis.

Thermal parameterization was performed using lithological profiles and complementary laboratory data from the BDGI and the national Soil and Rock Thermal Properties Database. A dedicated Python-based algorithm was developed to convert lithological data into point estimates of thermal conductivity and resistivity. These values were spatially interpolated using the Euclidean allocation method, which enabled the creation of continuous maps representing both average thermal conductivity calculated up to given depths and thermal resistivity determined at specific depths.

Depth intervals were selected to reflect the operating ranges of different subsurface applications. Maps of thermal con-

ductivity (2–30 m b.g.l.) correspond to the depth zones used by energy geostructures and horizontal ground heat exchangers, while thermal resistivity maps (2 and 5 m b.g.l.) represent the depth range relevant for underground transmission and distribution networks, including power cables, pipelines, and district heating systems. Together, these datasets offer an integrated perspective on the thermal environment of urban subsurfaces, linking geothermal potential to the performance and reliability of buried infrastructure (Źeruń et al., 2025).

The novelty of this study lies in establishing the first large-scale, data-driven workflow for deriving near-surface thermal properties from the national BDGI database, providing unprecedented spatial detail for city-scale vSGP assessment in Poland and offering a transferable framework for other urban areas with comparable geological datasets. The proposed approach demonstrates how existing engineering-geological data, originally collected for construction purposes, can be effectively repurposed for renewable energy planning and development. This research builds upon the preliminary concept introduced in Źeruń et al. (2024), where the feasibility of using the BDGI for shallow geothermal assessment was initially suggested. The present study extends that framework by implementing a complete computational workflow, expanding the analysis to include thermal resistivity alongside conductivity, and providing an in-depth interpretation of results in the context of Smart City energy management and underground infrastructure planning. This workflow provides a preliminary, city-scale assessment and does not replace site-specific methods such as thermal response tests (TRT) or laboratory measurements, which remain necessary at the design stage of geothermal installations.

OUTLINE OF GEOLOGICAL CONDITIONS

Warsaw is located in the Wisła River valley, within the central part of the Warsaw Trough, which was formed during the Quaternary Period. The left-bank section of the city lies within the boundaries of the glacial upland – an elevated, flat area dissected by the Wisła River along its eastern edge, descending sharply to the valley. The valley itself comprises two floodplain terraces and three terraces above present flood level (Sarnacka, 1992).

The stratigraphic profile of the Quaternary deposits in Warsaw includes fluvioglacial, glacial, and ice-dammed lake deposits from glaciation phases, as well as fluvial and organic deposits from interglacial phases. During the Holocene, the Vistula River accumulated a 1.5 metre thick sedimentary succession composed of fine-grained sands with interbedded silty and sandy-muddy layers. Oxbow areas contain peat and peaty aggradations exceeding 2 m in thickness. During the Dryas interval, dune formations developed, while Vistula river fluvial accumulations reached a thickness of 5 m and consisted of sands and gravels of varying grain sizes. Terrace areas were covered with compact clayey mud.

During the Pleistocene-Holocene transition, glacial uplands were mantled by loess-like silts and sandy eluvial deposits. Beneath these deposits lie Pliocene strata – predominantly clays – reaching 140 m in thickness. The top of the Pliocene was glaciectonically deformed. Below this unit, Miocene strata occur, composed mainly of sand, silt and clay with interbedded lignite seams tens of metres thick. Older formations include Oligocene marine clastic deposits (sand, silt, and clay, 50–80 m thick), forming a continuous cover above the Cretaceous rocks. The oldest known deposits in Warsaw comprise Cretaceous

marly strata, including marls and sandy marls, with the top of this sequence situated at depths of 260–290 m b.g.l. in the central Warsaw trough (Frankowski and Wysokiński, 2000).

In Warsaw and its surroundings, two main groundwater systems occur. The shallow Quaternary aquifer is composed mainly of sands from the Mazovian Interglacial, locally overlain by discontinuous glacial tills. The Quaternary aquifer lies at depths from a few to ~100 m, with variable thickness and geometry: thicker and more continuous in the Wisła Valley (up to 60 m) and more irregular on the upland west of the river. Beneath it, low-permeability Pliocene clays (50–120 m thick) separate the shallow groundwater from deeper levels. Below these, Miocene sands and silts (20–40 m thick) form a confined aquifer, underlain by Oligocene glauconitic marine sands (30–40 m thick, at depths of 180–270 m), which constitute the most important deeper groundwater reservoir of high quality. At greater depths, Cretaceous and Jurassic formations contain chloride-sodium mineral waters of varying salinity.

For urban planning and shallow geothermal potential assessment, only unconsolidated deposits, hereinafter referred to as soil in the engineering sense of this word (compressive strength R_c 600 kPa, according to ISO 14689), were considered, as lithified rock formations lie far below the depth range analysed, and have no influence on the very shallow geothermal potential studied.

MATERIALS AND METHODS

A detailed description of the BDGI structure and its application in urban-scale analyses was previously discussed by Żeruń et al. (2024). In this study, the database was restructured and integrated with the national Soil and Rock Thermal Properties Database to enhance the accuracy of parameterization and to enable comprehensive mapping of both thermal conductivity (λ) and resistivity (ρ). This integration forms the methodological foundation for the reproducible, multi-depth geothermal potential mapping presented herein.

DATA SOURCES – ENGINEERING-GEOLOGICAL DATABASE

The BDGI constitutes the largest digital collection of geoengineering data for major Polish urban agglomerations. It integrates geological, geotechnical and hydrogeological reports, along with borehole profiles. These datasets, developed within the framework of Engineering-geological maps of urban agglomerations (Fig. 1), contain between 15,000 and 50,000 records of shallow boreholes (typically 2–10 m deep) for each city. The borehole records serve as the basis for thematic maps that enable assessment of geoengineering conditions in urban areas – supporting spatial planning, forecasting, and investment decision-making (Frankowski et al., 2018). The BDGI datasets originate from standardized geotechnical and geological investigations conducted according to national and European guidelines, ensuring a high level of data consistency; however, local resolution varies with borehole density, as is typical of large archival datasets.

Borehole data, along with geotechnical soundings, are stored in the GeoSTAR software database, which is used for creating profiles, cross-sections, statistics, and 3D geological models. The database structure is composed of several relational tables (Fig. 2). The GS_Borehole table stores information on borehole location, depth, contractor, drilling date, and

method. The GS_Profile_Log contains lithostratigraphic descriptions, layer genesis, and their reclassification into engineering-geological units. This standardized structure enables the integration of archival and newly acquired data from both public and private sources. The system follows national and European soil and rock classification standards (Ryżyński and Nałęcz, 2016).

The BDGI, derived from GeoSTAR data, allows for the collection of geological and geotechnical information combined with laboratory test results. These data underpin regional subsurface characterization in urban areas and the creation of Engineering-geological maps, serving as essential reference material for GIS-based analyses and geostatistical modelling. By combining multiple digital layers, thematic maps are generated to synthesize lithological, stratigraphic and geotechnical information relevant for construction and spatial planning.

The full methodology for producing digital engineering-geological atlases is detailed in the document “Geological and engineering atlases of urban agglomerations at a scale of 1:10 000 – Instructional Document” (Judkowiak et al., 2021), available online at <https://www.pgi.gov.pl/inzynierska/1-geologia-inzynierska/gi-projekty/13168-baza-danych-geologiczno-inzynierskich.html#metodyka>.

All data compiled are accessible via PGI-NRI spatial data viewers, which enable visualization and download of borehole profiles, cross-sections, and engineering-geological maps in PDF format. The BDGI is therefore an invaluable tool for preliminary subsurface investigations, planning of in situ and laboratory testing, and enhancing the understanding of subsurface conditions in urban areas (Frankowski et al., 2020).

DATA SOURCES – SOIL AND ROCK THERMAL PROPERTIES DATABASE

The Soil and Rock Thermal Properties Database compiles laboratory measurements of effective thermal conductivity performed on mineral soil samples of varying water content and bulk density. The detailed testing methodology is described in Łukawska et al. (2020): “Serial Laboratory Effective Thermal Conductivity Measurements of Cohesive and Non-cohesive Soils for the Purpose of Shallow Geothermal Potential Mapping and Databases — Methodology and Testing Procedure Recommendations”. The database includes over 1000 soil (both cohesive and non-cohesive) and rock samples from different regions of Poland, holding over 6000 measurements of thermal conductivity (λ). Thermal resistivity (ρ) is the inverse of conductivity, so it can be assumed that the resistivity = $1/\lambda$.

Selected samples were tested across five water content ranges for non-cohesive soils and five liquidity index (IL – a geotechnical parameter describing the consistency and physical state of cohesive soils) ranges for cohesive soils, according to the national standard PN-B-02480:1986. Each soil type was represented by three subsamples.

For non-cohesive soils, thermal conductivity increases with increasing water content (Table 1). The most rapid growth occurs between 0–5% water content, slowing as pores become saturated. The highest λ values are observed under full water saturation (two-phase conditions). Among the soil types analysed, the lowest λ values were recorded for gravels (Ż) – from 0.22 W/m · K (0–5% water content) to 2.80 W/m · K (>20% water content), whereas the highest were found for sandy gravels with cobbles (Po) – from 0.42 W/m · K (0–5% water content) to 3.21 W/m · K (>20% water content).

For cohesive soils, λ values initially increase with water content (or saturation) and decrease beyond IL = 0.25 (Table 2).

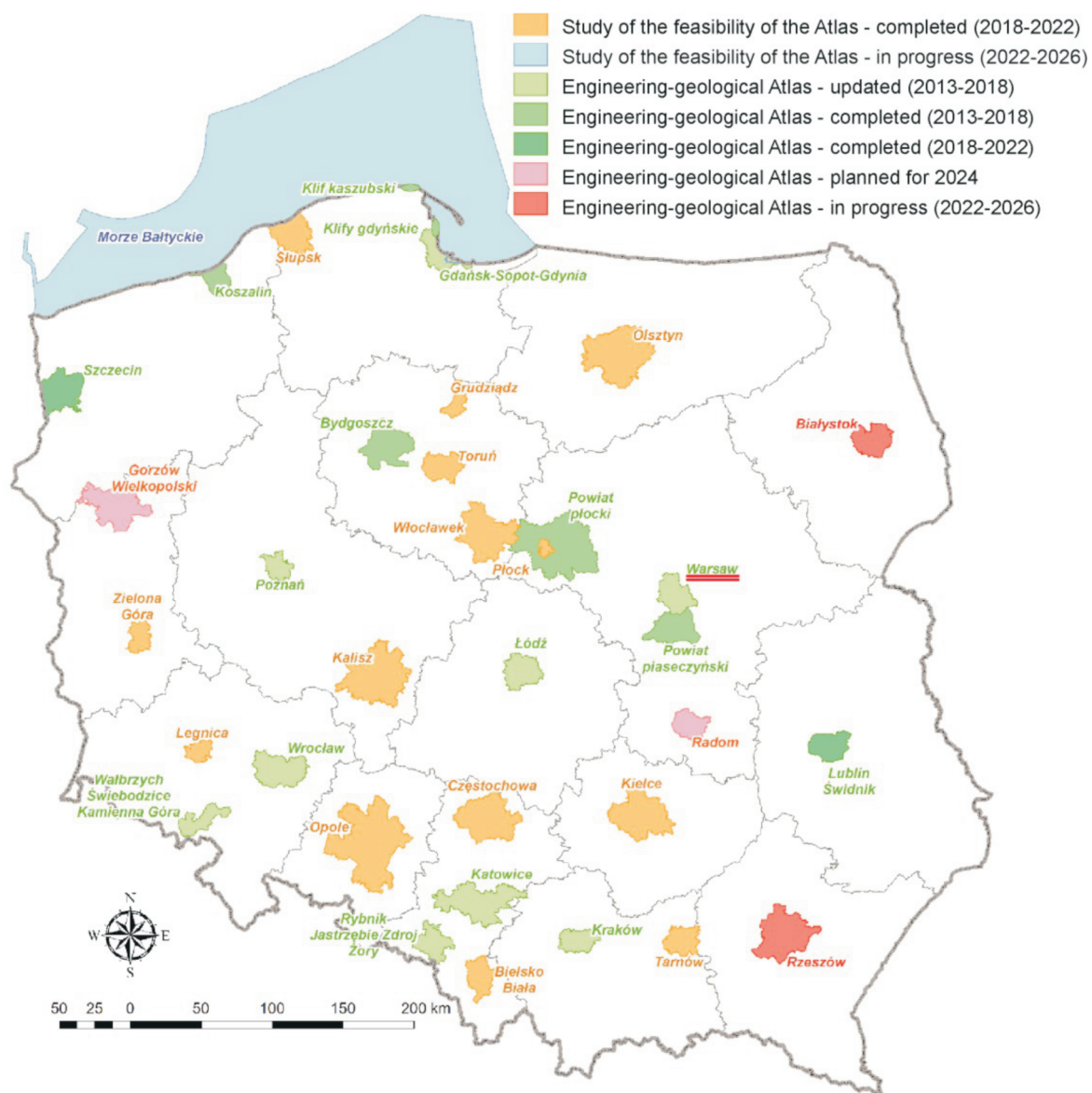


Fig. 1. Status of development of Engineering-geological atlases at 1:10 000 scale
 (source: geoportal.pgi.gov.pl/atlasy_gi/projekt/realizacja)

The highest values were observed for sandy clays (Pg) – up to $3.31 \text{ W/m} \cdot \text{K}$ at $0 < \text{IL} < 0.25$, while the lowest occurred for clays (I) – from $0.61 \text{ W/m} \cdot \text{K}$ ($\text{IL} < 0$) to $1.50 \text{ W/m} \cdot \text{K}$ ($0 < \text{IL} < 0.25$). All cohesive soil types show a decline in λ beyond $\text{IL} = 0.25$, reflecting increased water-induced structural changes that reduce effective thermal transfer.

The database also includes accompanying physical parameters: water content, bulk density, porosity, grain-size distribution, consistency limits, organic matter and carbonate content, simplified mineralogy, genesis, stratigraphy, and sample coordinates. Together, these datasets constitute the empirical foundation for the thermal parameterization of geological layers within the BDGI framework, supporting the semi-automatic mapping of thermal conductivity and resistivity in the Warsaw case study.

PARAMETERIZATION ALGORITHM

To generate geothermal potential maps for the very shallow subsurface (up to 30 m b.g.l.), a dedicated parameterization and mapping workflow was developed. The process integrates geological and geotechnical data from the BDGI with thermal property data from the Soil and Rock Thermal Properties Database. The parameterization stage consists of four sequential steps (Fig. 3), forming the analytical foundation for subsequent spatial processing of continuous thermal conductivity and resistivity layers in the GIS environment.

Compared to the initial workflow outlined by Żeruń et al. (2024), the present version introduces several significant improvements. These include:

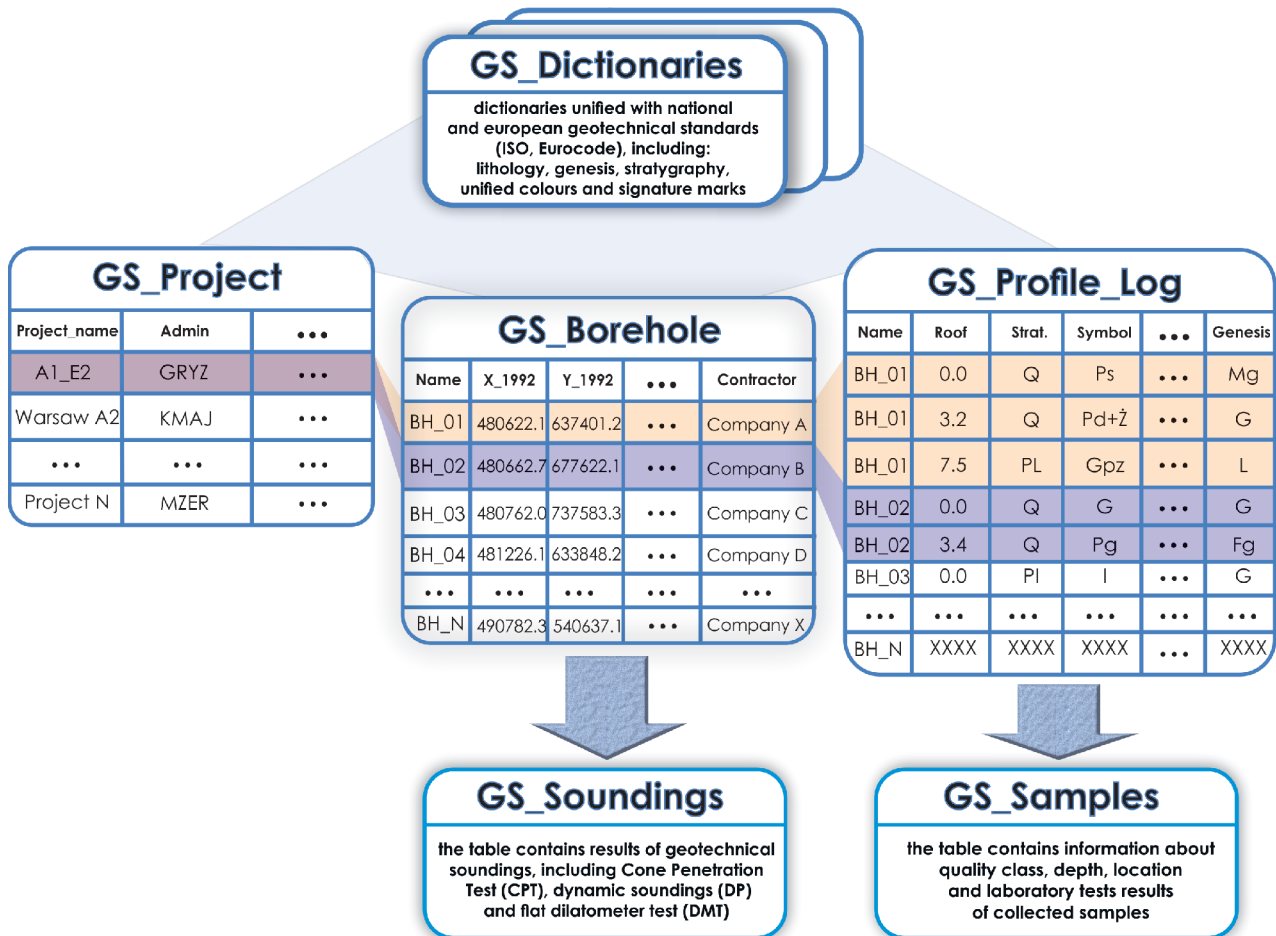


Fig. 2. A simplified scheme of the GeoSTAR borehole data base structure (Ryżyński and Nalecz, 2016)

- simultaneous computation of “up-to-depth” conductivity and “at-depth” resistivity parameters,
- implementation of groundwater correction for non-cohesive layers,
- optimization of data merging between geological and thermal datasets.

These modifications enable more accurate characterization of lithological variability and enhance the resolution of the resulting thermal maps. The computational workflow was implemented in Python using standard scientific libraries (NumPy, Pandas), without incorporating third-party algorithms or external code repositories such as GitHub; all algorithmic components were developed internally as part of PGI-NRI’s proprietary analytical framework.

STEP 1 DATA QUERY FROM BDGI

The workflow begins with data extraction from the BDGI database, which provides comprehensive geological, stratigraphic and geotechnical information. Two primary relational tables were used: GS_BOREHOLES (metadata such as coordinates, elevation, depth, drilling date, and documentation details) and GS_PROFILE_LOG (lithology, genesis, stratigraphy, groundwater level, and results of physical-mechanical soil test

ing). For the Warsaw region, 35,000 borehole records were available, generating 166,000 distinct lithological intervals requiring parameterization.

STEP 2 THERMAL ADAPTATION FOR LITHOLOGICAL UNITS

Each unique lithological unit was assigned representative thermal properties – primarily thermal conductivity (λ) and thermal resistivity (ρ) – derived from the national Soil and Rock Thermal Properties Database. The assignment was based on lithology, genesis and stratigraphic position. The values were adjusted according to individual soil characteristics such as water content, bulk density and compaction. In layers with admixtures or interbeds, the final parameter value was computed as a weighted average of both lithologies, using predefined correction coefficients reflecting the type and proportion of interlayering.

STEP 3 INTEGRATION OF GEOLOGICAL AND THERMAL DATASETS

The adapted thermal parameters were then merged with geological data from BDGI, creating a unified dataset that combines lithological and thermal attributes. Hydrogeological cor-

Table 1

Effective thermal conductivity (λ) for non-cohesive soils depending on water content (after Łukawska et al., 2021)

Soil classification according to PN-B-02480:1986	Water content [%]														
	0 - 5			5 - 10			10 - 15			15 - 20			> 20		
	λ min	λ max	λ̄ λ	λ min	λ max	λ̄ λ	λ min	λ max	λ̄ λ	λ min	λ max	λ̄ λ	λ min	λ max	λ̄ λ
P _π Piasek pylasty	0.28	1.80	1.06	1.66	2.11	1.86	1.82	2.25	2.14	2.23	2.67	2.54	2.60	2.88	2.76
P _d Piasek drobny	0.24	1.81	1.08	1.70	2.16	1.90	1.87	2.42	2.17	2.39	2.75	2.66	2.63	2.90	2.77
P _s Piasek średni	0.28	1.86	1.11	1.72	2.21	1.95	1.93	2.45	2.20	2.41	2.90	2.73	2.88	3.12	3.03
P _r Piasek gruby	0.25	1.89	1.12	1.74	2.25	2.00	1.98	2.46	2.27	2.39	2.83	2.70	2.71	3.01	2.85
P _o Pospółka	0.42	2.01	1.26	1.82	2.31	2.19	2.10	2.56	2.33	2.55	2.92	2.62	2.81	3.21	3.05
ż Żwir	0.22	1.76	1.03	1.61	2.00	1.84	1.95	2.37	2.15	2.27	2.61	2.30	2.54	2.80	2.67

Symbol description: min – lowest measured effective thermal conductivity value [W/m K]; max – highest measured effective thermal conductivity value [W/m K]; λ̄ – arithmetic mean value of effective thermal conductivity for a certain soil type [W/m K].

Soil classification based on particle size distribution according to PN-B-02480:1986:

P: 0.05–2.00 mm: 68 ± 90%; 0.002–0.05 mm: 10 ± 30%; <0.002 mm: 0 ± 2%;

Pd: >2 mm: <10%; >0.5 mm: <50%; >0.25 mm: <50%;

Ps: >2 mm: <10%; >0.5 mm: <50%; >0.25 mm: >50%;

Pr: >2 mm: <10%; >0.5 mm: >50%;

Po: <0.002 mm: <2%; >2 mm: 10–50%;

ż: <0.002 mm: <2%; >2 mm: >50%

Table 2

Effective thermal conductivity (λ) for cohesive soils according to liquidity index classes (after Łukawska et al., 2021)

Soil classification according to PN-B-02480:1986	Liquidity index IL [-]														
	IL < 0			IL ≤ 0			0 < IL ≤ 0,25			0,25 < IL ≤ 0,50			0,50 < IL ≤ 1,00		
	λ min	λ max	λ̄ λ	λ min	λ max	λ̄ λ	λ min	λ max	λ̄ λ	λ min	λ max	λ̄ λ	λ min	λ max	λ̄ λ
π Pył	0.61	1.40	1.25	1.10	1.91	1.71	1.80	2.31	2.10	1.60	2.10	1.90	1.41	1.91	1.71
P _g Piasek gliniasty	0.71	1.61	1.45	2.10	2.86	2.71	2.41	3.31	3.06	2.00	2.80	2.56	1.91	2.51	2.31
G _p Glina piaszczysta	1.01	2.10	1.90	2.01	2.61	2.46	2.41	2.90	2.76	2.00	2.61	2.31	1.71	2.31	1.80
G Glina	0.91	1.81	1.41	1.51	2.41	2.21	1.80	2.60	2.34	1.70	2.20	1.85	1.41	1.91	1.70
G _π Glina pylasta	0.81	1.41	1.20	1.21	2.01	1.86	1.60	2.41	2.21	1.41	2.00	1.70	1.21	1.60	1.46
I Ił	0.61	1.01	0.86	0.61	1.26	1.11	1.11	1.50	1.36	0.90	1.31	1.10	0.75	1.16	1.01

Symbol description: min – lowest measured effective thermal conductivity value [W/m K]; max – highest measured effective thermal conductivity value [W/m K]; λ̄ – arithmetic mean value of effective thermal conductivity for a certain soil type [W/m K].

Soil classification based on particle size distribution according to PN-B-02480:1986:

: 0.05–2.00 mm: 0 ± 30%; 0.002–0.05 mm: 60 ± 100%; <0.002 mm: 0 ± 10%;

Pg: 0.05–2.00 mm: 60 ± 98%; 0.002–0.05 mm: 0 ± 30%; <0.002 mm: 2 ± 10%;

Gp: 0.05–2.00 mm: 50 ± 90%; 0.002–0.05 mm: 0 ± 30%; <0.002 mm: 10 ± 20%;

G: 0.05–2.00 mm: 30 ± 60%; 0.002–0.05 mm: 30 ± 60%; <0.002 mm: 10 ± 20%;

G_π: 0.05–2.00 mm: 0 ± 30%; 0.002–0.05 mm: 50 ± 90%; <0.002 mm: 10 ± 20%;

I: 0.05–2.00 mm: 0 ± 50%; 0.002–0.05 mm: 0 ± 50%; <0.002 mm: 30 ± 100%

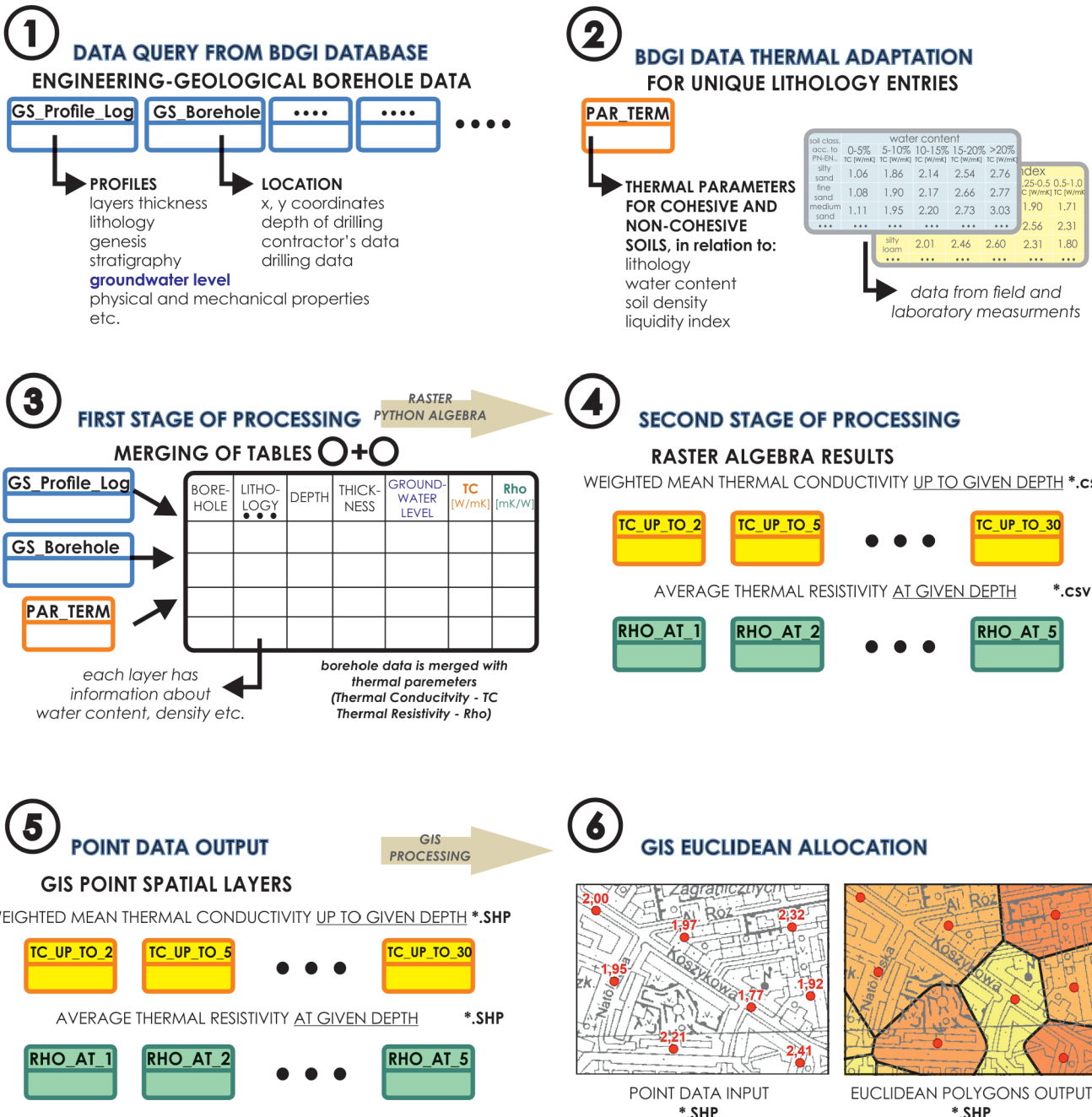


Fig. 3. Parameterization process – steps 1–6

rections were introduced for non-cohesive soils located below the groundwater table, reflecting fully saturated conditions. The presence and depth of the groundwater table are critical for estimating vSGP (Zhao et al., 2022; Rammler et al., 2023). When the groundwater table intersects a non-cohesive layer, the stratum is subdivided into saturated and unsaturated zones, each with distinct thermal conductivity. As groundwater levels may fluctuate over time, the values recorded during drilling represent the best available information; despite this temporal uncertainty, incorporating the documented water table provides a

more accurate thermal parameterization than omitting hydrogeological effects altogether. After this correction, weighted average thermal conductivities are calculated for the lithological profiles down to predefined depths. The weighting algorithm follows the methodology described by Klonowski et al. (2020), ensuring that each depth interval reflects the cumulative influence of soil layering and moisture conditions. In parallel, thermal resistivity values are determined at defined cut-off levels (2 and 5 m b.g.l.). The algorithm identifies the geological layer present at the specified depth and assigns its resistivity value. This pro-

vides a point-specific estimate of thermal conditions at these depths without applying vertical averaging.

STEP 4 RASTER ALGEBRA AND TABULAR OUTPUT

Using raster algebra operations, two distinct thermal parameters were computed:

- a) average thermal conductivity up to a given depth,
- b) thermal resistivity at a given depth.

The output was compiled into tabular form, where each borehole location was associated with its calculated parameter values. This dataset constituted the analytical base for spatial representation in the GIS environment.

GIS ANALYSIS

The GIS analysis stage transforms the parameterized numerical results into continuous spatial representations of subsurface thermal properties. This part of the workflow focuses on geostatistical processing and cartographic presentation. The procedure includes three main steps: steps 5 to 7 (Figs. 3 and 4), leading from the tabular data to the final visual outputs.

STEP 5 POINT DATA OUTPUT

The tabular dataset containing thermal conductivity and resistivity values was converted into a vector point layer (SHP format). Each borehole was represented as a spatial point carrying calculated thermal attributes for predefined depths. This conversion enabled subsequent spatial allocation and map generation.

STEP 6 GIS EUCLIDEAN ALLOCATION

To transform discrete point data into continuous polygonal coverage, the Euclidean allocation method was applied. This geostatistical technique assigns each location in space to the nearest data point (borehole) based on straight-line distance, generating a set of polygons of equal proximity. Polygon boundaries are automatically placed midway between neighbouring boreholes, ensuring objective and reproducible spatial partitioning. Although the input dataset consists of vector points, the Euclidean Allocation tool performs the computation in raster space and the results were subsequently converted back to vector polygons for mapping.

Only boreholes deeper than 2 m were included in this step to maintain geological reliability and exclude superficial, non-representative data. At greater depths, polygons corresponding to areas without borehole information were automatically excluded. The resulting polygons were subsequently aggregated into 0.2 W/m · K thermal conductivity classes and equivalent resistivity ranges, producing a consistent basis for thermal mapping.

STEP 7 FINAL MAP LAYOUTS

The final stage involves integrating Euclidean polygons with a topographic base map of Warsaw to produce the thermal parameter maps (Fig. 4). These include:

- a) maps of weighted-average thermal conductivity up to a given depth,
- b) maps of thermal resistivity at specific depths (e.g., 2 and 5 m).

The visual outputs depict the spatial distribution of thermal properties within the upper 30 m of the subsurface and provide a foundation for assessing local geothermal potential. The Euclidean allocation method ensures transparency, objectivity and reproducibility, which are key advantages in heterogeneous urban datasets with uneven borehole coverage.

RESULT INTERPRETATION AND DISCUSSION

The thermal conductivity and resistivity maps generated for Warsaw provide the first high-resolution assessment of the vSGP for an urban area in Poland. Their interpretation reveals key spatial and depth-related patterns that have direct implications for both geothermal energy utilization and the management of underground infrastructure.

INTERPRETATION OF THERMAL RESISTIVITY PATTERNS

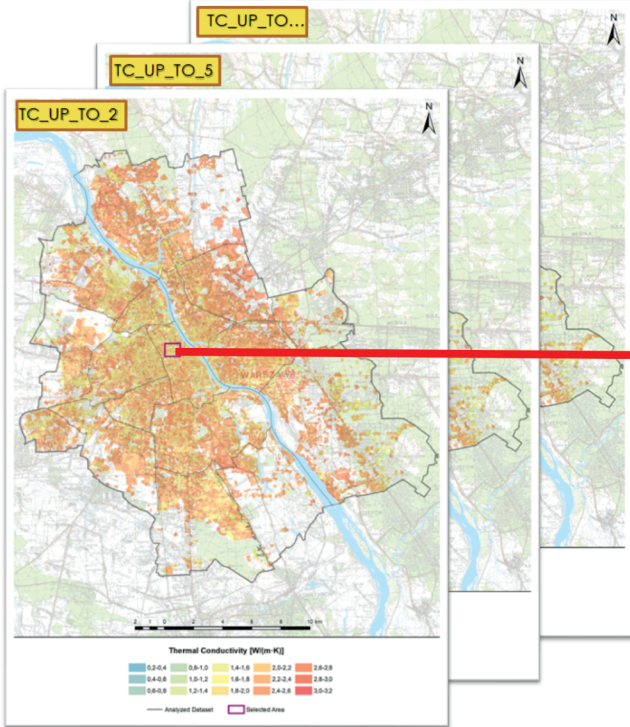
The thermal resistivity maps generated for 2 and 5 m below the ground level reflect the spatial variability of the unconsolidated Quaternary deposits prevalent in Warsaw. These layers are composed predominantly of sandy and silty deposits with variable moisture content and compaction, while cohesive soils and anthropogenic fills occur locally. The calculated resistivity values at 2 m depth range from ~0.3 to over 3.0 m · K/W, with the most extensive zones (almost 60% of the area) characterized by very low resistivity (0.5–0.7 m · K/W) (Fig. 5). These zones are mainly distributed within river valleys and areas with shallow groundwater tables, where higher saturation and fine-grained materials enhance thermal coupling. This relationship forms one of the key controls on the spatial distribution of thermal resistivity in the study area. Depths (2 and 5 m b.g.l.) correspond to typical installation levels of underground utility networks in Warsaw, making thermal resistivity directly relevant for assessing heat dissipation and operational conditions of buried infrastructure.

At 5 m depth, the range of thermal resistivity values remains similar, but the spatial distribution becomes more uniform, reflecting both increasing soil compaction and more stable hydrogeological conditions with depth. The share of areas with very low resistivity (<0.5 K · m/W) rises, accounting for nearly three-quarters of the total area, indicating improved heat transfer potential. Higher thermal resistivity values (0.85–1.5 m · K/W) occur locally, for example, in areas where sandy deposits with low moisture content and significant admixtures of anthropogenic materials dominate.

From a practical standpoint, these resistivity maps support the design and monitoring of underground utility networks – electric power cables, gas pipelines and water mains – where soil resistivity directly affects thermal performance, energy losses and safe operational limits. Areas characterized by very low resistivity represent optimal zones for efficient heat transfer and reduced thermal stress on buried infrastructure. These zones therefore represent priority areas for efficient thermal management of underground utility systems.

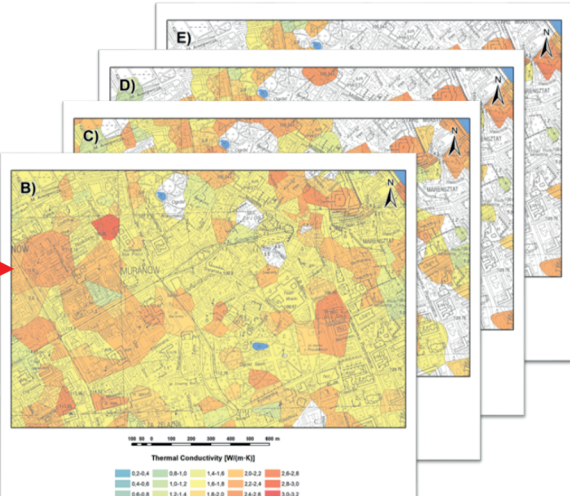
7 FINAL MAP LAYOUTS

WEIGHTED MEAN THERMAL CONDUCTIVITY MAPS UP TO GIVEN DEPTH



LAYOUT
SYMBOLISATION
*.LYR

GIS POLYGON
SPATIAL LAYERS
*.SHP



LAYOUT
SYMBOLISATION
*.LYR

GIS POLYGON
SPATIAL LAYERS
*.SHP

AVERAGE THERMAL RESISTIVITY MAPS AT GIVEN DEPTH

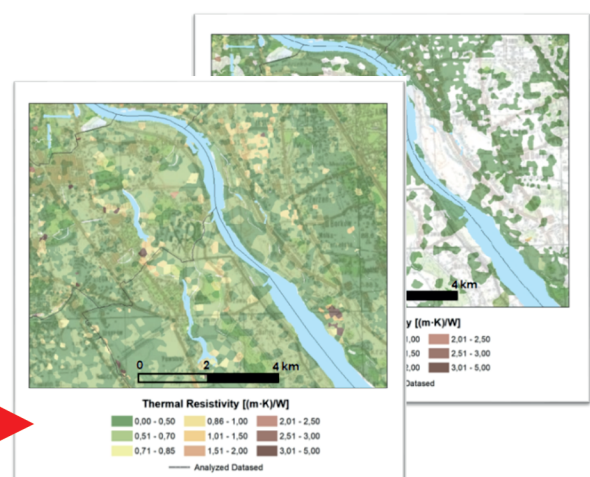
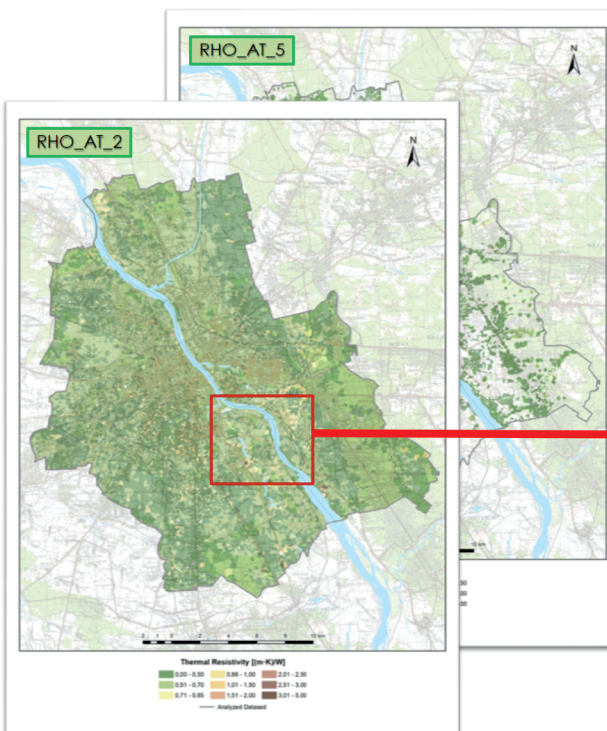


Fig. 4. Parameterization process – final map layouts (Step 7)

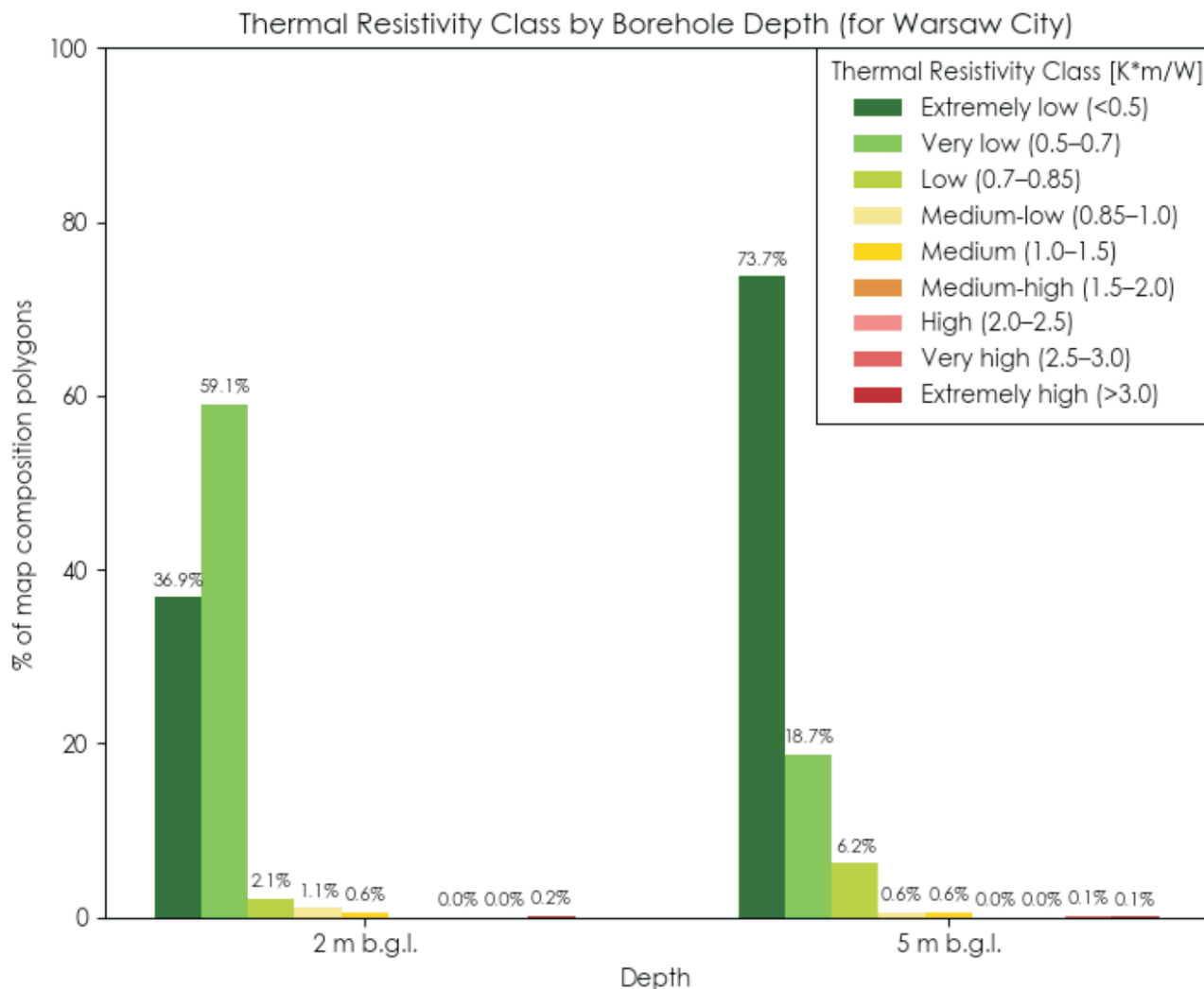


Fig. 5. Thermal resistivity distribution at 2 and 5 m b.g.l.

INTERPRETATION OF THERMAL CONDUCTIVITY PATTERNS

The weighted-average thermal conductivity () maps, produced for cumulative intervals down to 2, 5, 10, 15, 20, 25, and 30 m b.g.l., show a systematic increase in λ with depth (Fig. 6). The mean conductivity for the top 2 m layer is 1.65 W/m · K, rising to 2.55 W/m · K for the interval up to 30 m. This vertical trend reflects the transition from loose, variably moist surface soils to more compact, denser, and frequently saturated deposits.

Spatially, higher λ values (>2.2 W/m · K) occur predominantly in the eastern districts along the Vistula river terraces, where coarse sands and gravels prevail. Lower λ values (<1.7 W/m · K) dominate the western and north-western parts of the city, where cohesive Pliocene clays and silts form the uppermost strata. The variability of λ diminishes with depth, which confirms that the lithological and moisture-related heterogeneity typical of the near-surface zone gradually decreases in deeper soil layers.

For geothermal engineering, these findings indicate that large parts of Warsaw provide favourable conditions for vSGE

exploitation. Conductivity values exceeding 2.0 W/m · K are sufficient for efficient operation of both horizontal ground heat exchangers and thermoactive geostructures such as energy piles, diaphragm walls, and tunnel linings. The gradual increase in λ with depth also suggests stable long-term thermal performance and limited risk of efficiency loss due to seasonal temperature fluctuations or drying of surface layers. This makes deeper thermal zones particularly favourable for reliable and predictable operation of shallow geothermal systems.

INTEGRATED INTERPRETATION AND ENGINEERING IMPLICATIONS

The combined analysis of thermal conductivity () and thermal resistivity () demonstrates that Warsaw's subsoil generally offers a stable and conductive medium suitable for both energy extraction and thermal management. The correspondence between low resistivity and high conductivity zones corroborates the robustness of the parameterization and validates the geological logic of the mapping procedure.

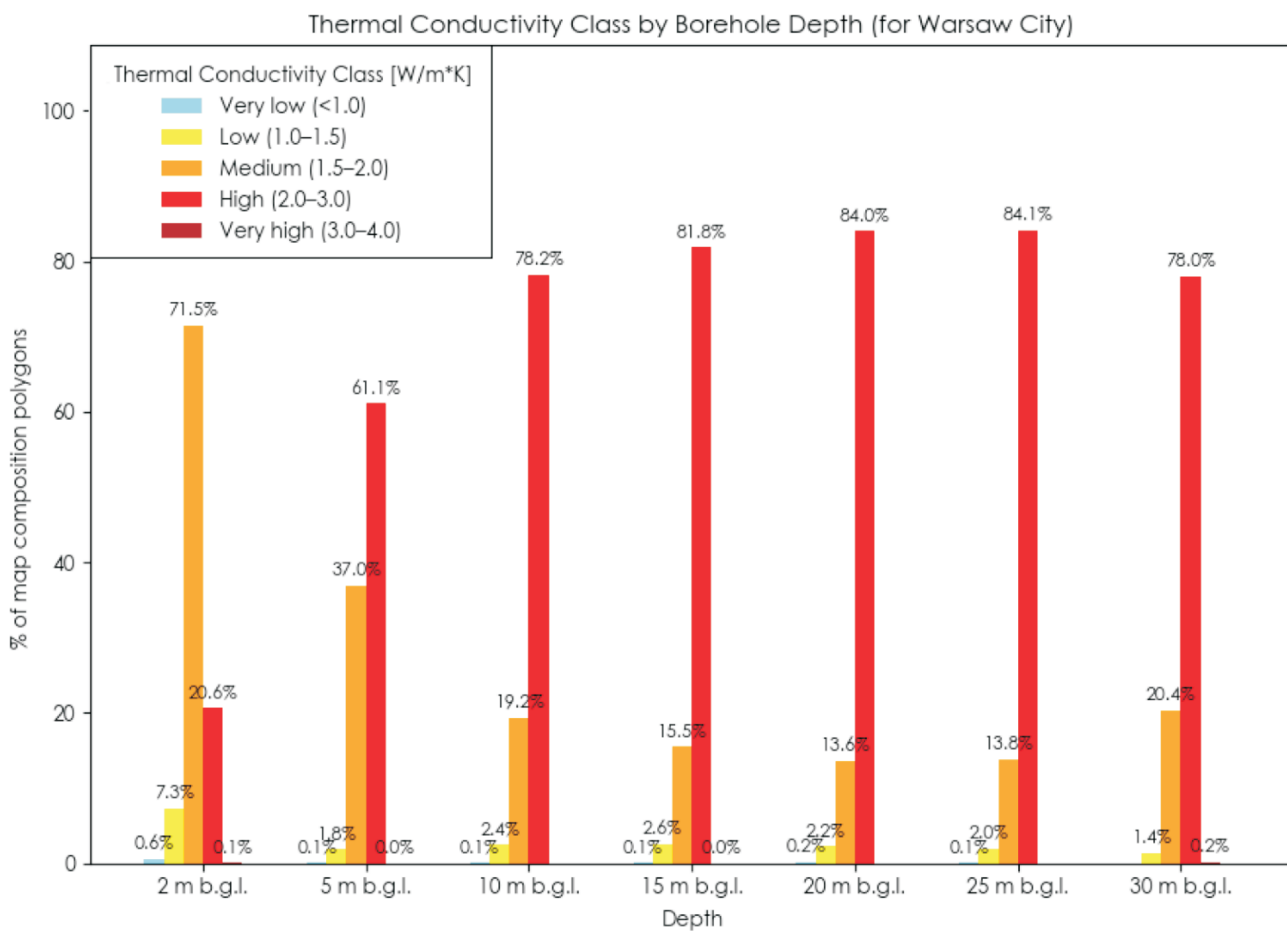


Fig. 6. Thermal conductivity distribution up to 2, 5, 10, 15, 20, 25, and 30 m b.g.l.

The “at-depth” thermal resistivity maps are particularly important for shallow underground infrastructure, as they indicate how effectively the local ground can dissipate or absorb heat. They can guide routing decisions for power transmission cables, inform the placement of energy-efficient district heating networks, and support thermal backfill design. The “up-to-depth” conductivity maps, by contrast, serve as a valuable reference for the preliminary design of geothermal systems operating within the upper 30 m b.g.l., particularly energy geo-structures integrated into buildings and transport infrastructure.

The spatial patterns identified in this study may also inform sustainable urban planning. Areas with high and low values correspond to zones of increased geothermal potential and may be prioritised for renewable energy installations or pilot projects under municipal Smart City strategies. Conversely, zones with low and high should be treated with caution, as they imply limited heat exchange efficiency and potentially higher system costs.

The spatial relationships observed in the current study confirm and extend the patterns identified in the earlier pilot analysis (Żeruń et al., 2024). In particular, the strong correlation between groundwater occurrence and zones of reduced thermal resistivity reinforces the validity of the parameterization procedure. Unlike the preliminary version, the present research pro-

vides a quantitative evaluation of spatial coverage, uncertainty assessment related to borehole distribution, and an explicit discussion of engineering implications for energy and infrastructure planning.

METHODOLOGICAL CONSIDERATIONS AND LIMITATIONS

The Euclidean allocation algorithm applied in this research offers several methodological advantages. It provides a deterministic and transparent means of delineating zones of influence between boreholes, avoiding the subjective interpretation inherent to conventional interpolation methods. This approach ensures reproducibility and facilitates clear communication of results to non-specialists and decision-makers.

Nevertheless, the approach has limitations that stem primarily from the heterogeneity and unequal distribution of borehole data. The density of available data decreases markedly below 20 m b.g.l., reducing spatial resolution and increasing geological uncertainty. While the Euclidean allocation method preserves the geometric consistency of polygon boundaries across depth levels, this consistency may lead to overgeneralization in areas with sparse input data. Future work should ad-

dress these limitations through hybrid approaches combining deterministic allocation with probabilistic uncertainty assessment.

BROADER IMPLICATIONS AND PROSPECTS

Beyond geothermal energy applications, the workflow described can contribute to the integrated thermal management of the urban subsurface. The same datasets can be used to assess the risk of heat accumulation in densely developed districts, simulate underground temperature fields, which are crucial for the soil shear strength described by [Yavari et al. \(2016\)](#), or evaluate the interaction between geothermal systems and buried utilities.

The Warsaw case study demonstrates the feasibility of repurposing engineering-geological data for energy transition objectives. The methodology is scalable and can be readily adapted to other Polish cities covered by the BDGI. With supplementary datasets, it can be extended to derive additional thermal parameters (such as specific heat capacity or thermal diffusivity) and, in the future, to generate near-surface ground temperature maps.

The integration of such spatial information with urban energy models will enhance the capability of planners and designers to make data-driven decisions supporting low-carbon development. As digital geological repositories continue to expand, the coupling of parameterized datasets with machine-learning techniques will enable continuous improvement of predictive accuracy and regional transferability of the results.

CONCLUSIONS AND FURTHER RESEARCH

This study builds upon and substantially extends the initial framework proposed by [Źeruń et al. \(2024\)](#), presenting a fully developed and validated methodology for mapping the vSGP of urban areas using engineering-geological data. The developed workflow combines lithological parameterization with GIS-

based Euclidean allocation, enabling the visualization of thermal conductivity and resistivity consistently and transparently. The Warsaw case study confirms that large parts of the city possess favourable thermal properties — moderate to high conductivity and low resistivity — suitable for efficient operation of energy geostructures and shallow heat exchange systems.

The methodology bridges the gap between traditional geological mapping and energy system planning, offering a data-driven tool to support Smart City strategies and sustainable underground space management. By avoiding subjective interpolation and maintaining geometric consistency across depth levels, the approach ensures reproducibility and clear communication of results to engineers, planners and public stakeholders.

Given the unified structure of the BDGI, the workflow can be readily extended to other urban areas, with only minor adjustments for regional lithological conditions. In most regions of the Polish Lowlands, the shallow geological structure down to ~30 m b.g.l. is relatively uniform and only weakly influenced by tectonic processes, allowing the workflow to be applied with minimal adjustments. However, in areas where tectonic faults or contacts between distinct structural units occur, such as southern Poland, additional subdivision criteria or algorithmic refinements may be required to correctly reflect geological boundaries. Future developments will focus on improving parameter prediction through the application of machine-learning regression algorithms, and on expanding the framework towards the generation of additional thermal parameter maps, including specific heat capacity and near-surface ground temperature. Together, these advancements will enhance the precision, scalability, and practical applicability of geothermal potential assessments in support of Poland's low-carbon energy transition.

Acknowledgments. This article was financed by the National Fund for Environmental Protection and Water Management.

This paper is an extended version of our paper published in the proceedings of the 49th Workshop on Geothermal Reservoir Engineering, Stanford University, Stanford, California, USA, February 12-14, 2024

REFERENCES

Baralis, M., Barla, M., Bogusz, W., Donna, A.D., Ryzyński, G., Źeruń, M., 2018. Geothermal potential of the NE extension Warsaw (Poland) metro tunnels. *Environmental Geotechnics*, **7**: 282–294; <https://doi.org/10.1680/jenge.18.00042>

Barla, M., Di Donna, A., Baralis, M., 2020. City-scale analysis of subsoil thermal conditions due to geothermal exploitation. *Environmental Geotechnics*, **7**: 306–316; <https://doi.org/10.1680/jenge.17.00087>

Ciapała, B., Georgiou, G.S., Aresti, L., Onoufriou, T., Florides, G.A., Christodoulides, P., 2025. Thermal performance evaluation of energy piles and energy foundations: a comprehensive review of thermal effectiveness testing methods. *Energy & Buildings*, **346**, 116181; <https://doi.org/10.1016/j.enbuild.2025.116181>

Enescu, D., Colella, P., Russo, A., Porumb, R.F., Seritan, G.C., 2021. Concepts and methods to assess the dynamic thermal rating of underground power cables. *Energies*, **14**, 2591; <https://doi.org/10.3390/en14092591>

Frankowski, Z., Wysokiński, L., 2000. Atlas geologiczno-inżynierski Warszawy (in Polish). CAG, Pol. Geol. Inst. – NRI, Warszawa. Inv number: 2070/2000.

Frankowski, Z., Majer, E., Sokołowska, M., Ryzyński, G., Ostrowski, Sz., Majer, K., 2018. Engineering geological research conducted in the Polish Geological Institute during the last fifty years of activity (in Polish with English summary). *Przegląd Geologiczny*, **66**: 752–768;

Frankowski, Z., Majer, E., Sokołowska, M., Ryzyński, G., Ostrowski, Sz., Majer, K., 2020. Development of engineering geology at the Polish Geological Institute (in Polish with English summary). *Przegląd Geologiczny*, **68**: 345–355.

Goetzel, G., Burns, E.R., Stumpf, A.J., Lin, Y., Kolker, A., Kłonowski, M., Steiner, C., Cahalan, R.C., Pepin, J.D., 2023. City-Scale Geothermal Energy Everywhere to Support Renewable Resilience – a Transcontinental Cooperation, *PROCEEDINGS*, 48th Workshop on Geothermal Reservoir Engineering, Stanford University, Stanford, California.

Górecki, W. (ed.), Szczepański, A., Sadurski, A., Hajto, M., Pałpiernik, B., Kuźniak, T., Kozdra, T., Soboń, J., Szewczyk, J.,

Sokołowski, A., Strzelenski, W., Haładus, A., Kania, J., Kurzydłowski, K., Gonet, A., Capił, M., Śliwa, T., Ney, R., Kępińska, B., Bujakowski, W., Rajchel, L., Banaś, J., Solarzki, W., Mazurkiewicz, B., Pawlikowski, M., Nagy, S., Szamałek, K., Feldman-Olszewska, A., Wagner, R., Kozłowski, T., Malenta, Z., Sapińska-Śliwa, A., Sowiżdżał, A., Kotyza, J., Leszczyński, K.P., Ganczar, M., 2006a. *Atlas of Geothermal Resources of Mesozoic Formations in the Polish Lowlands*. AGH University of Science and Technology in Krakow. Ministry of Environment, NFE&WM in Warsaw.

Górecki, W. (ed.), Szczepański, A., Sadurski, A., Hajto, M., Papiernik, B., Szewczyk, J., Sokołowski, A., Strzelenski, W., Haładus, A., Kania, J., Rajchel, L., Feldman-Olszewska, A., Wagner, R., Leszczyński, K.P., Sowiżdżał, A., 2006b. *Atlas of Geothermal Resources of Paleozoic Formations in the Polish Lowlands*. AGH University of Science and Technology in Krakow. Ministry of Environment, NFE&WM in Warsaw.

Górecki, W. (ed.), Szczepański, A., Oszczypko, N., Hajto, M., Oszczypko-Clowes, M., Papiernik, B., Kępińska, B., Czopek, B., Haładus, A., Kania, J., Banaś, J., Kurzydłowski, K., Rożniatowski, K., Solarzki, W., Mazurkiewicz, B., Kuźniak, T., Machowski, G., Michna, M., Soboń, J., Luboń, W., Pełka, G., Rajchel, L., Sowiżdżał, A., Kotyza, J., Capił, M., Hałaj, E., Harasimiołuk, M., Bujakowski, W., Barbacki, A., Hołojuch, G., Kasztelewicz, A., Pająk, Ł., Tomaszewska, B., Chowaniec, J., Zuber, A., Malata, T., Augustyńska, J., Operacz, T., Freiwald, P., Patorski, R., Witek, K., Czerwińska, B., Gaśior, E., Ślimak, C., Wartał, W., Skupień, M., Goryl, M., Cichoń, K., Kudrewicz, R., Budzisz, P., Zaźreżynska, J., Dowgiałło, J., 2011. *Atlas of Geothermal Waters and Energy Resources in the Western Carpathians*. AGH University of Science and Technology in Krakow. Ministry of Environment, NFE&WM in Warsaw.

Górecki, W. (ed.), Sowiżdżał, A., Jasnos, J., Papiernik, B., Hajto, M., Machowski, G., Kępińska, B., Czopek, B., Kuźniak, T., Kotyza, J., Luboń, K., Pełka, G., Zajac, A., Szczepański, A., Haładus, A., Kania, J., Banaś, J., Solarzki, W., Mazurkiewicz, B., Zubrzycki, A., Luboń, K., Peryt, T., Barbacki, A., Pająk, Ł., Tomaszewska, B., Harasimiołuk, M., Kurzydłowski, K., Nowak, J.J., Latour, T., Czerwińska, B., Kudrewicz, R., Szewczyk, J., 2012. *Geothermal Atlas of the Carpathian Foredeep*. AGH University of Science and Technology in Krakow. Ministry of Science and Higher Education Republic of Poland, the National Science Centre.

Górecki, W. (ed.), Hajto, M., Augustyńska, J., Jasnos, J., Kuśmirek, J., Kuźniak, T., Machowski, G., Machowski, W., Nosal, J., Michna, M., Papiernik, B., Sowiżdżał, A., Stefańiuk, M., Szczygieł, M., Wachowicz-Pyzik, A., Ząbek, G., Rajchel, L., Lemberger, M., Czop, M., Haładus, A., Kania, J., Szczepański, A., Golonka, J., Banaś, J., Mazurkiewicz, B., Solarzki, W., Capił, M., Porowski, A., Oszczypko, N., Ostrowski, C., Targosz, P., Wojdyła, M., Barbacki, A., Bielec, B., Bujakowski, W., Hołojuch, G., Kasztelewicz, A., Kępińska, B., Miecznik, M., Pająk, Ł., Skrzypeczak, R., Tomaszewska, B., Budzisz, P., Zaźreżynska, J., Herman, Z., Harasimiołuk, M., Czerwińska, B., Kublik, B., Pasek, P., Palychuk, U., Chowaniec, J., Szewczyk, J., Baran, U., Kudrewicz, R., Borsukiewicz-Gozdur, A., Nowak, W., Wisniewski, S., Kurzydłowski, K., Kalandyk, K., 2013. *Geothermal Atlas of the Eastern Carpathians*. AGH University of Science and Technology in Krakow. Ministry of Science and Higher Education Republic of Poland, the National Science Centre.

Hou, G., Taherian, H., Song, Y., Jiang, W., Chen, D., 2022. A systematic review on optimal analysis of horizontal heat exchangers in ground source heat pump systems. *Renewable and Sustainable Energy Reviews*, 154, 111830; <https://doi.org/10.1016/j.rser.2021.111830>

Judkowiak, M., Samel, I., Majer, E., Sokołowska, M., Majer, K., 2021. Problems and challenges in Engineering and Geological Database maintenance (p-BDGI) (in Polish with English summary). *Przegląd Geologiczny*, 69: 772–778.

Klonowski, M., Ryzyński, G., Żeruń, M., Kocyła, J., 2020. Evaluation and statistical interpretation of low-temperature geothermal energy potential for selected locations in Poland. *Geological Quarterly*, 64: 506–514; <https://doi.org/10.7306/gq.1534>

Loveridge, F., McCartney, J.S., Narsilio, G.A., Sanchez, M., 2020. Energy geostructures: A review of analysis approaches, in situ testing, and model scale experiments. *Geomechanics for Energy and the Environment*, 22, 100173; <https://doi.org/10.1016/j.gete.2019.100173>

Łukawska, A., Ryzyński, G., Żeruń, M., 2020. Serial laboratory effective thermal conductivity measurements of cohesive and non-cohesive soils for the purpose of shallow geothermal potential mapping and databases – methodology and testing procedure recommendations. *Energies*, 13, 914; <https://doi.org/10.3390/en13040914>

Łukawska, A., Żeruń, M., Ryzyński, G., 2021. Influence of moisture content of mineral soils on the value of effective thermal conductivity based on the results of laboratory measurements (in Polish with English summary). *Przegląd Geologiczny*, 69: 604–610; <https://doi.org/10.7306/2021.34>

Rammler, M., Zeh, R., Bertermann, D., 2023. Influence of Groundwater on the Very Shallow Geothermal Potential (vSGP) in the Area of a Large-Scale Geothermal Collector System (LSC). *Geosciences*, 13, 251; <https://doi.org/10.3390/geosciences13080251>

Ryzyński, G., Nałęcz, T., 2016. Engineering-geological data model – the first step to build a national Polish standard for multilevel information management. *World Multidisciplinary Earth Sciences Symposium (WMESS 2016)*, 44, 032025; <https://doi.org/10.1088/1755-1315/44/3/032025>

Ryzyński, G., Kozdrój, W., Szłasa, M. (eds.), 2023. *Instrukcja wykonywania map potencjału i uwarunkowań środowiskowych geotermii niskotemperaturowej* (in Polish). Państwowy Instytut Geologiczny – Państwowy Instytut Badawczy, Warszawa.

Sarnacka, Z., 1992. Stratigraphy of Quaternary sediments of Warsaw and its vicinity (in Polish with English summary). *Prace Państwowego Instytutu Geologicznego*, 138: 1–36.

Yavari, N., Tang, A.M., Pereira, J.M., Hassen, G., 2016. Effect of temperature on the shear strength of soils and the soil–structure interface. *Canadian Geotechnical Journal*, 53: 1186–1194; <https://doi.org/10.1139/cgj-2015-0355>

Zhao, Z., Lin, Y.F., Stumpf, A., Wang, X., 2022. Assessing impacts of groundwater on geothermal heat exchangers: a review of methodology and modeling. *Renewable Energy*, 190: 121–147; <https://doi.org/10.1016/j.renene.2022.03.089>

Żeruń, M., Jagoda, E., Majer, E., Łukawska, A., Majer, K., Ryzyński, G., Samel, I., 2024. Adaptation of the Engineering-Geological Database for Very Shallow Geothermal Potential Mapping of the Urban Areas. Case study: Warsaw. *PROCEEDINGS, 49th Workshop on Geothermal Reservoir Engineering*, Stanford University, Stanford, California.

Żeruń, M., Jagoda, E., Majer, E., Wczelik, K., Ryzyński, G., 2025. Criteria for assessing the suitability of the subsurface for heat storage using closed systems (BTES, PTES/TTES, EF) (in Polish with English summary). *Przegląd Geologiczny*, 73: 666–673; <https://doi.org/10.7306/2025.72>